3-D localization of gamma ray sources with coded apertures for medical applications

I Kaissas[1], C Papadimitropoulos[2], K Karafasoulis[3], C Potiriadis[1] and C P Lambropoulos[2]
[1]Greek Atomic Energy Commission, Greece
[2]Technological Educational Institute of Sterea Ellada, Greece
[3]Hellenic Army Academy, Greece

E-mail:lambrop@mail.teiste.gr

Abstract. Several small gamma cameras for radioguided surgery using CdTe or CdZnTe have parallel or pinhole collimators. Coded aperture imaging is a well-known method for gamma ray source directional identification, applied in astrophysics mainly. The increase in efficiency due to the substitution of the collimators by the coded masks renders the method attractive for gamma probes used in radioguided surgery. We have constructed and operationally verified a setup consisting of two CdTe gamma cameras with Modified Uniform Redundant Array (MURA) coded aperture masks of rank 7 and 19 and a video camera. The 3-D position of point-like radioactive sources is estimated via triangulation using decoded images acquired by the gamma cameras. We have also developed code for both fast and detailed simulations and we have verified the agreement between experimental results and simulations. In this paper we present a simulation study for the spatial localization of two point sources using coded aperture masks with rank 7 and 19.

Introduction

In cancer surgery, intraoperative localization of spots of radio-traced tissues is implemented by gamma counter probes or more sophisticated handheld gamma cameras [1]. For instance, sentinel nodes with diameter from 0.8 to 1.5 cm are traced with ^{99m}Tc injection in order to identify and remove the cancerous ones with intraoperative use of handheld detectors [2]. Due to the physiology of lymphs and pharmacokinetics, ^{99m}Tc occupies only a small portion of the entire node. Also due to the anatomy of lymphatic system, these nodes are spaced apart more than a couple of centimeters. Considering ^{99m}Tc concentrations as point-like sources, in this study we investigate the use of two CdTe pixelated detectors with coded apertures and the combination of their images with the triangulation method in order to locate point-like radioactive sources in 3-D space. Application in radioscintigraphy of one gamma camera with a coded mask has been investigated recently [3].

Materials, definitions and methods

Simulations and measurements are employed to evaluate the imaging capabilities of an integrated system that consists of two energy dispersive and position sensitive detectors and a coded aperture (or mask) mounted on top of each detector. The mask-to-detector distance b and the spacing between the two detectors d are adjustable with b_{min}=18mm and $d_{\min}$=17cm due to the detector housing. These two

parameters (b_{min}, d_{min}) specify a minimum distance for normal operation (z_{min}=7.82cm) where the intraoperative procedure can record a clear signature of the source on both detectors.

Each position sensitive detector is an array of 4×2 hybrids made by pixelated CdTe chips, 1mm thick, bump-bonded to pixel readout electronics in the form of Application Specific Integrated Circuit (ASIC) which record the charge delivered to each pixel. The active area of the detector is 4.4×4.4 cm^2 and has 16384 pixels with 350um pitch. The system can record signals from 15keV up to 200keV with 1KeV step and with 3-4 keV FWHM energy resolution as reported in [4] and verified by measurements with ^{241}Am, ^{57}Co and ^{99m}Tc. The absorption efficiency of the 1mm thick CdTe at 140KeV is 30%. The results reported below are from data both experimental and simulated taken with a 10mCi ^{241}Am source 1mm in diameter.

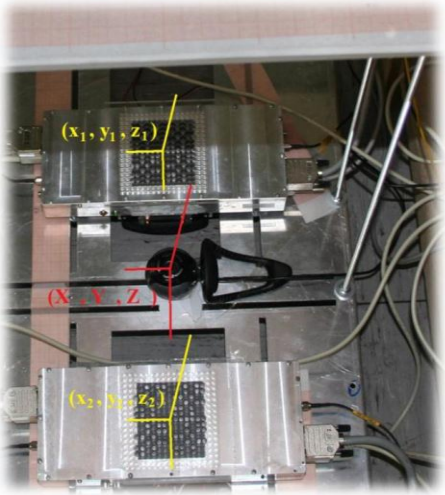

Figure 1. A view of the system. The two gamma cameras with coded apertures mounted on an aluminum base, can be seen together with a web-camera. The image also depicts the co-ordinate systems (x_i, y_i, z_i), i=1,2 of the two cameras used to extract the displacement of their SPSF, as well as the system reference frame (X,Y,Z).

For the experimental setup (figure 1) we have constructed two pairs of MURA coded apertures with Ranks 7 and 19, respectively. In Table 1 their main characteristics are outlined. Both masks have been constructed on a PMMA (Plexiglas) sheet where a grid of holes is drilled according to the mask rank. Thus, for Rank 7 the holes were 5.6mm in diameter and of 3mm pitch while for Rank 19 they were 2mm and 1mm, respectively. Each hole is filled with cylindrical blocks (Rank 7) or spheres (Rank 19) according to the MURA mask pattern. The size of the mask and the detector defines a solid angle, which is known as Fully Coded Field of View (FCFOV). A radioactive source within the FCFOV illuminates the mask and projects a fraction of its pattern (shadowgram) onto the detector surface. Since two detectors are utilized, a system FCFOV (denoted as $FCFOV_S$ hereafter) is introduced as the common area of the FCFOV of the detectors and is directly related to both their separation *d* and the mask-to-detector distance *b*. For $Z>z_{min}$ the $FCFOV_S$ is 77.71×77.71 degrees.

The recorded shadowgram (figure 2) is the result of the convolution of the source with the mask as photons pass through the transparent and opaque elements [5],[6]. The applied method of deconvolution is by cross-correlating the shadowgram with a special function G, essentially a replica of the mask pattern itself. This function utilizes balanced correlation along with digital reconstruction to minimize artifacts [6]. The result of cross-correlation, denoted as *rec matrix*, defines the Source Point Spread Function (SPSF). Its peak corresponds to the trace of the source in pixel coordinates providing a signature of the source direction [7]. The displacement of the SPSF peak r_i ($SPSF_i$) from the center of the coordinate system (x_i, y_i, z_i) of the i_{th} detector (figure 1) designates the azimuthal angle (φ_i) while the elevation angle θ_i is calculated as $\theta_i=\text{atan}(r_i/b)$. This set of parameters (φ_i, θ_i)

Table 1. Main characteristics of the two experimental MURA masks

Rank	Number of elements	Diameter of elements (mm)	Surface (mm^2)	Grid pitch (mm)
7	13×13	5.6	72.8×72.8	3
19	37×37	2.0	74.0×74.0	1

specifies a unique direction that originates from the $SPSF_i$ and passes through the mask center. The triangulation algorithm gives the estimated coordinates of the radioactive source in the system reference frame (X, Y, Z). Given the set of parameters (φ_i, θ_i) from the reconstructed images, the algorithm finds the middle point of the minimum distance vector that is perpendicular to the two lines (figure 3).

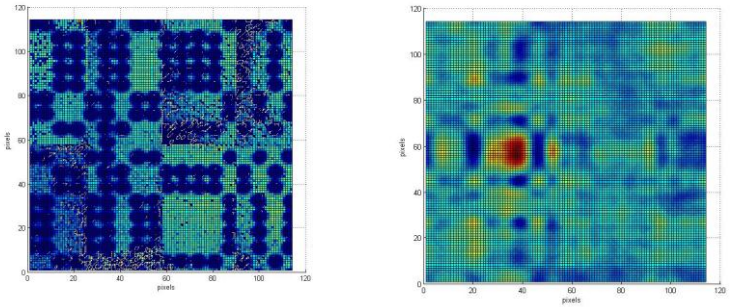

Figure 2. Recorded shadowgram (left) and the result of the deconvolution (rec matrix, right) with a clear signature of the SPSF (red spot).

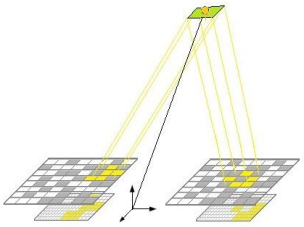

Figure 3. A schematic diagram that depicts the triangulation algorithm.

Results – discussion – conclusions

The Point Source Location Accuracy (PSLA) [8] and the Angular Resolution (AR) [9] are the figures of merit for the instrument. PSLA specifies how close the estimated location is to the actual position of the source while the AR defines the minimum angle where two sources can be clearly separated and identified. Both parameters have been estimated via Monte Carlo simulations.

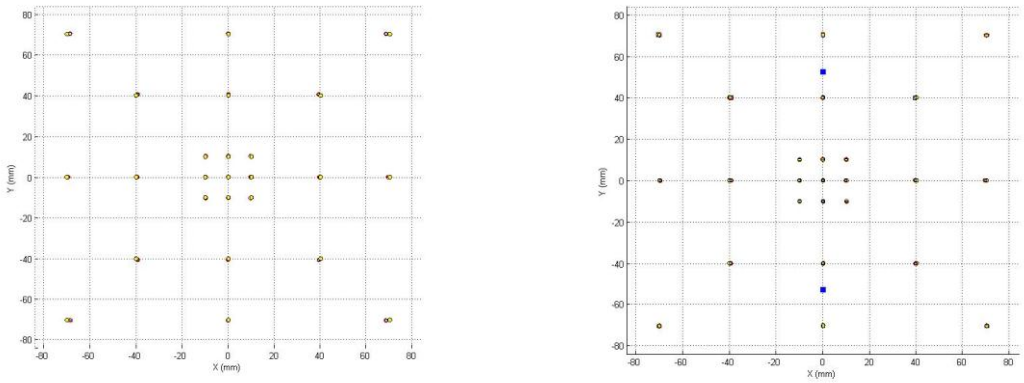

Figure 4. Source positions (yellow spots) projected in XY plane and their corresponding estimation (red boxes) at Z=150mm for Ranks 19 (left) and 7 (right), respectively. Blue squares indicate the actual position of the detectors.

In order to evaluate the PSLA with respect to MURA rank 7 and 19 masks, a ^{241}Am point-like source was positioned at several locations within the $FCFOV_S$ but at the same elevation Z=150mm (figure 4). The simulation experiment was iterated 50 times for each position. Table 2 shows some indicative results where the source location is estimated with high accuracy. With a mask to detector distance of 10mm, the AR of two point-like sources is 17.7^o (figure 5) for Rank 7 and 12^o for Rank 19. This gives minimum spacing between the two sources 48mm for the rank 7 and 32mm for the rank 19, at Z=150mm. When the size of the element of the rank 19 mask is changed to 1.85mm and the mask to detector distance becomes 18mm, then the angular resolution becomes 6.5^o (figure 6), which at Z=110mm gives a minimum spacing of 12.5mm.

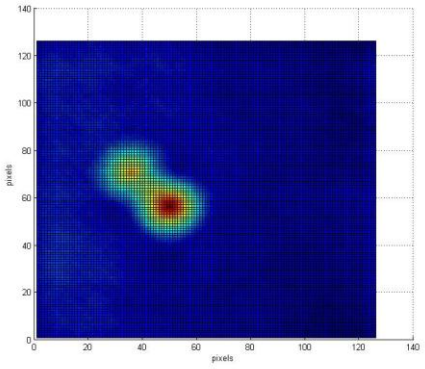

Figure 5. the result of reconstruction of two point like sources at Z=150mm with a mask of rank 7 and with element size 5.6mm

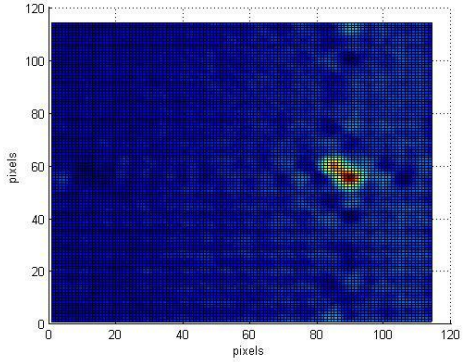

Figure 6. The result of reconstruction of two point like sources at Z=110mm with a mask of rank 19 and with element size 1.85mm

Triangulation gives the capability of 3-D localization, but it has no significant effect on the spatial resolution of the system, because the angular resolution of each mask-detector system determines the final system resolution. Further increase of the rank of the mask will result to higher spatial resolution.

Table 2. Indicative parameters for source location X=0, Y=0, Z=150mm.

Parameter	Rank 19	Rank 7	Unit
Total counts per detector	~33500	~37000	-
SNR per detector	34±2	31±2.7	-
X_{est} (@ 95% confidence level)	-0.09036 ± 0.3825	-0.0066 ± 0.4144	mm
Y_{est} (@ 95% confidence level)	0.06128 ± 0.3910	0.02180 ± 0.5101	mm
Z_{est} (@ 95% confidence level)	148.78 ± 0.6142	149.72 ± 1.7226	mm

Acknowledgement
This research has been funded by the ESA Contract 4200014240 «CdTe crystallization and related compounds» and by the FP7-SEC-218000 COCAE project.

References
[1] Tsuchimochi M., Hayama K. 2013 *Physica Medica* **29** 126
[2] Jeong S H, Baek H C, Son I Y, Cho Y D, Chung K M, Min Y J, Ko H Y and Kim T B 2006 *J. Korean Med. Sci.* **21** 865
[3] F Hirofumi, Idoine D J, Gioux S, Accorsi R, Slochower R D, Lanza C R and Frangioni V J 2012 *Mol. Imaging Biol* **14** 173
[4] Meng L.J., Tan J.W., Spartiotis K., Schulman T. 2009, *Nucl. Instr. Meth. Phys. Res. A* **604** 548
[5] Anderson N D, Stromswold C D, Wunschel C S, Peurrung J A and Hansen R R 2006, *Technometrics* **48**, no. 2 252
[6] Lees E J, Bugby L S, Bassford J D, Blackshaw E P and Perkins C A 2013, *J. Inst.* **8** 10021
[7] Fenimore E E and T. M. Cannon M T 1981 *Applied Optics* **20** 10 1858
[8] Gmar M., Agelou M., Carrel F., Schoepff V. 2011 *Nucl. Instr. Meth. Phys. Res. A* **652** 638
[9] Caroli E, Stephen B J, Cocco D G, Natalucci L and Spizzichino A 1987 *Space Sci. Rev.* **45** 349
[10] Gros A, Goldwurm A, Cadolle-Bel M, Goldoni P, Rodriguez J, Foschini L, Santo D M and Blay P 2003 *Astronomy & Astrophysics* **411** 179